Journal of Alloys and Compounds 501 (2010) 297–300

Contents lists available at ScienceDirect

Journal of Alloys and Compounds

journal homepage: www.elsevier.com/locate/jallcom

Study of Fe-rich FePt nanoparticles synthesized by a single step reverse micelle route

S.S. Kalyan Kamal[a,*], P.K. Sahoo[a], L. Durai[a], P. Ghosal[a], S. Ram[b], Manivel Raja[a]

[a] Defence Metallurgical Research Laboratory, Hyderabad 500058, India
[b] Materials Science Centre, Indian Institute of Technology Kharagpur, Kharagpur 721302, India

ARTICLE INFO

Article history:
Received 6 December 2009
Received in revised form 14 April 2010
Accepted 15 April 2010
Available online 24 April 2010

Keywords:
FePt nanoparticles
Magnetization
Mössbauer
TEM

ABSTRACT

Fe-rich FePt nanoparticles with an average size of 5 nm were prepared using a reverse micelle route. As synthesized FePt powders were disordered face centered cubic in structure. DSC thermogram displays phase transformation at 575 °C, based on which heat treatments were carried in the temperature range of 500–600 °C. XRD patterns show that the degree of ordering increased with the increase in heat treatment temperature. An utmost coercivity of 3.2 kOe was observed for 600 °C heat-treated sample. The *M–H* loops were asymmetric in nature suggesting the presence of a second phase, Fe-oxide (Fe_3O_4) that is also observed from the XRD patterns. Mössbauer spectra reveals that on heat treatment the super-paramagnetic phase transforms into an ordered face centered tetragonal phase. The presence of 23% super-paramagnetic phase even after heat-treating at 600 °C reveals that the phase transformation is incomplete.

1. Introduction

Synthesis and characterization of magnetic nanoparticles with controlled size, distribution and composition has gained importance because of their potential applications in diverse fields such as ferrofluids, biosensing, magnetic storage devices and drug delivery [1–4]. Binary alloy systems like FePt, CoPt and FePd have been in special focus because of their long range ordering with high magnetocrystalline anisotropy (K_u) of 4–7 × 10^7 erg/cm^3 [5,6], which is very important for high-density storage media. Chemically ordered FePt alloys with $L1_0$ structure are highly sought after materials as they exhibit remarkable magnetic properties based on their size and form. The high magnetocrystalline anisotropy of the face centered tetragonal phase permits a reduction in size of nanoparticles (NPs) below 10 nm while retaining the stability of their magnetization against thermal fluctuations and demagnetizing effects. The high value of K_u also defers the emergence of super-paramagnetic limit well into terabit/in^2.

Ever since Sun et al. [7] reported the synthesis of stable FePt NPs by a chemical route, lot of focus has been laid on production of monodispersed FePt NPs with uniform particle size and good chemical stability. To obtain near equiatomic FePt NPs various solution based chemical routes have been explored such as polyol process [8,9], thermal decomposition [10], chemical reduction [11], and reverse micelle techniques [12]. Though the chemically synthesized FePt NPs have the advantage of uniform particle size and ease of synthesis, unfortunately the as synthesized NPs are face centered cubic (fcc) in structure which do not exhibit the magnetocrystalline anisotropy. In order to obtain the desired face centered tetragonal (fct) structure the NPs have to be heat-treated. The heat treatment procedure however results in undesirable coalescing and sintering of the NPs, which in turn inhibits the direct application of chemically prepared FePt NPs. Many efforts have been made in the direction of realizing the application of chemically synthesized FePt NPs some of which include direct synthesis of fct phase materials [13], or reducing the phase transformation temperature of FePt NPs by doping with coinage metals like Cu and Ag [14]. Others include modified sintering techniques [15,16] and synthesis of surface modified FePt NPs such as core shell structures [17,18], which reduces the adverse effects of sintering at higher temperatures. The FePt/Fe-oxide core–shell structures reported earlier [19] use the Fe-oxide shell as a barrier for the equiatomic FePt NPs from coalescence at higher temperatures. Though a lot of work has been focused on the synthesis and heat treatment procedures of equiatomic FePt NPs, the cost effect of Pt makes it very difficult for their commercialization; hence a need arises to bring down the Pt content but yet retaining a reasonable value of coercivity so that they could be used in recording media. In this paper we report a single step reverse micelle technique for synthesis of FePt NPs with Fe-rich composition and study the effect of excess Fe content on the crystal structure, sintering and magnetic properties of both the as synthesized and heat-treated samples.

* Corresponding author. Tel.: +91 040 24586779; fax: +91 040 2434 0884.
E-mail addresses: kalyanchem@dmrl.drdo.in, kalyanchem03@rediffmail.com (S.S. Kalyan Kamal).

0925-8388/$ – see front matter © 2010 Elsevier B.V. All rights reserved.
doi:10.1016/j.jallcom.2010.04.091

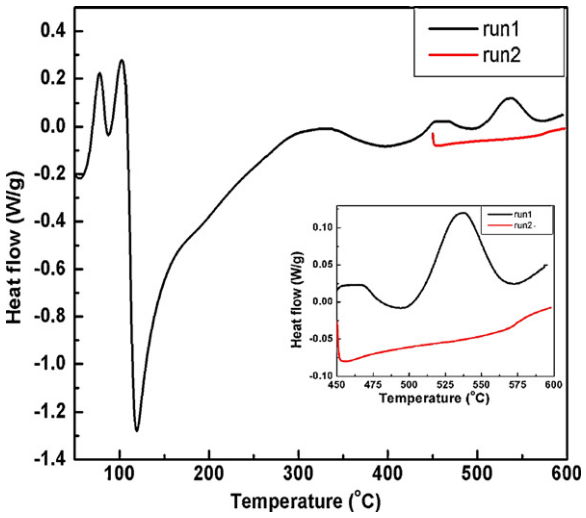

Fig. 1. DSC thermograms of the as synthesized FePt nanoparticles.

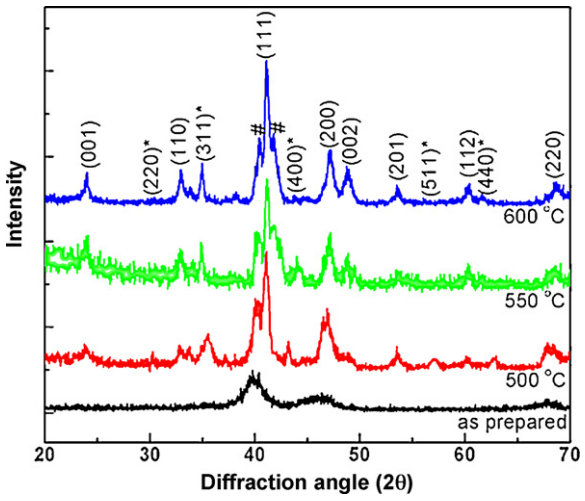

Fig. 2. XRD patterns of FePt nanoparticles obtained in as synthesized and heat-treated conditions (500–600 °C).

2. Experimental

2.1. Materials

All the chemicals were used as received. Platinum hexachloride hydrate ($PtCl_6{\cdot}H_2O$, 99.5%), ferric chloride ($FeCl_3$) (99.5%), cetyltrimethyl ammonium bromide (CTAB, 98%), n-butanol (95%), potassium borohydride (KBH_4, 98%), n-heptane (99%), and acetone (99%) were obtained from Alfa Aesar laboratories, India.

2.2. Method

A quaternary reverse micellar route described elsewhere [12] was used to synthesize FePt nanoparticles (NPs), except for that a Fe-rich composition was chosen instead of equiatomic ratio. In a typical synthesis 0.15 g of $PtCl_6{\cdot}H_2O$ and 0.10 g of $FeCl_3$ were dissolved in 10 ml of high pure water with 18.2 MΩ-cm electrical resistivity, obtained from Euro water purification system, CTAB was used as a surfactant, n-butanol as co-surfactant and potassium borohydride as reducing agent. The ratio of Fe and Pt precursors were chosen in such a way to obtain a Fe-rich composition. The NPs were separated from the solution by placing a $SmCo_5$ hard magnet beneath the glass beaker, which facilitates easy separation of the NPs from the solution. Once all the particles have collected at the bottom, leaving a clear solution at the top, the solvent was decanted. The NPs were washed twice using ethanol. Chemical characterization of the as synthesized powders was carried out using a portable X-ray fluorescence (XRF) spectrometer (Oxford-XMET 3000 XT). To know the behaviour of powders on exposure to higher temperatures, thermal profiles were carried out using a differential scanning calorimeter (DSC, TA-instruments Q100) and crystallographic phases were analyzed using an X-ray diffractometer (XRD, Philips PW3020) with Cu Kα radiation of wavelength 1.5418 Å as X-ray source. Magnetic characterization of the sample was carried out using a vibrating sample magnetometer (VSM, ADE-EV9) and to study the distribution of Fe in the crystal lattice of FePt NPs Mössbauer spectroscopy was carried out using a constant acceleration spectrometer with 25 mCi, ^{57}Co (Rh) radioactive source. The experimental spectra were analyzed using PCMOSS-II software. Size, morphology and distribution of the as synthesized NPs were examined using a transmission electron microscope (TEM, FEI, G2 Technai 20) at an accelerating voltage of 200 KV.

3. Results and discussion

XRF analysis of the as synthesized FePt NPs showed that the composition was Fe-rich as expected, because the concentrations of precursors taken was higher in Fe content and the composition is $Fe_{60}Pt_{40}$. Fig. 1 shows the thermograms of the as synthesized powders obtained from DSC. In Fig. 1, lot of endothermic peaks could be observed, the peaks at 87 and 118 °C could be attributed to the loss of solvent molecules ethanol and cosurfactant butanol respectively which have adhered to the NPs. A broad peak in the region of 320–400 °C arises due to the slow decomposition of organic moieties of the surfactant CTAB. A peak at 475 °C could possibly due to sintering of Fe-oxides and an endothermic peak with change in slope at 575 °C could be assigned to the order–disorder phase transformation. In order to confirm this, a second scan in the region of 450–600 °C was carried out on the same powders and it was observed that all the peaks except the one at 575 °C have disappeared as shown in Fig. 1 inset. This indicates that the peak arises from order–disorder phase transformation and therefore further incremental heat treatments were carried out at 500, 550 and 600 °C.

To carry out heat treatments the powders were packed in titanium foils and vacuum sealed in quartz tubes which were later subjected to heating in a muffle furnace at a heating rate of 10 °C/min. The samples were allowed to hold at the desired temperature for 1 h each and later were water quenched to room temperature. Fig. 2 shows XRD of as synthesized and heat-treated samples at different temperatures. From Fig. 2 it is clear that the as synthesized sample comprises of three broad peaks at 2θ values of 40.01°, 46.19° and 67.97°, which can be assigned to the disordered face centered cubic (fcc) reflections of the planes (1 1 1), (2 0 0) and (2 2 0) respectively. The heat-treated samples show more complicated patterns when compared to the as synthesized sample. The (1 1 1) peak becomes much sharper than that observed in as synthesized powders and shifted slightly to the right hand side by one degree to 41.06°, whereas the (2 0 0) peak starts to show a split with increase in heat treatment temperature and clearly resolves into two separate peaks (2 0 0) and (0 0 2) at 600 °C. This split indicates that the disordered fcc structure has transformed into a face centered tetragonal structure. The peaks at 23.88° and 33.09° start appearing at 500 °C and increase in intensity with increase in temperature, these two peaks can be assigned to the superlattice reflections (0 0 1) and (1 1 0) respectively of $L1_0$ structure. Fundamental peaks can be obtained from all fcc based materials but the superlattice reflections are obtained only from the regions of ordered material, this indicates that the disordered structure has transformed into a more ordered phase. In order to know the degree of ordering the (2 0 0) and (0 0 2) peaks of 600 °C heat-treated sample were deconvoluted and c/a ratio was calculated and the decrease in a-parameter with increase in Fe content from the equiatomic composition is in good agreement with earlier reported values [20]. A c/a value of 0.971 obtained from the d-spacing ratio and order parameter (S) value of 0.66 calculated from the relative intensities using the formula $S = [\{I(0\,0\,1)/I(1\,1\,1)\}_{exp}/\{I(0\,0\,1)/I(1\,1\,1)\}_{cal}]$ indicates incomplete ordering. The other peaks marked with '( )*' can be discerned to the (2 2 0), (3 1 1), (4 0 0), (5 1 1) and (4 4 0) reflections obtained from the iron oxide (Fe_3O_4) JCPDS 89-0691. Apart from the

Table 1
Mössbauer parameters of FePt nanoparticles obtained from least-square fitting.

Sample ID	Sub-spectra	Phase type	H_{hf} (kOe)	I.S. (mm/s)	Q.S. (mm/s)	Intensity (%)
As-prepared	Sextet	fcc	299 (2.5)	0.15 (0.04)	0.04 (0.05)	30 (5)
	Doublet	Super-paramagnetic	–	0.22 (0.01)	0.71 (0.03)	70 (3)
600 °C heat treated	Sextet	$L1_0$	285 (2.1)	0.18 (0.03)	0.20 (0.06)	57 (4)
	Doublet 1	Super-paramagnetic	–	0.42 (0.01)	0.90 (0.04)	23 (3)
	Doublet 2	Fe-oxide	–	0.95 (0.02)	1.95 (0.04)	20 (4)

Note: Values given in parentheses are the standard deviations.

Fe_3O_4 peaks other oxide forms were also detected from XRD which are marked with # at 40.41° and 41.77° which can be attributed to Fe_2O_3 and FeO respectively. This is consistent with the excess Fe present in the sample, which has a tendency to pick up oxygen and convert into oxide form.

Fig. 3 shows the *M–H* curves obtained from VSM for both as synthesized and heat-treated samples. From Fig. 3 it is clear that the as synthesized powders showed soft magnetic behaviour. As the heat treatment temperature was increased from 500 to 550 °C and subsequently to 600 °C the hysteresis loops opened up to yield higher coercivity (H_c) values of 0.5, 2.5 and 3.2 kOe but all the loops were not saturated at the applied field of 2 T. Though no great change is observed in the normalized magnetization values at a field of 2 T (M/M_{2T}), the coercivity values showed a very significant change with increased temperatures and this is consistent with XRD patterns showing a much ordered structure at 600 °C and also the order-disordered transformation peak from the DSC lying around 575 °C. All the heat-treated samples showed multiphase hysteresis loops which could be attributed to the presence of two phases in the material of which one being hard magnetic while the other soft magnetic. The soft magnetic phase being the Fe-oxides arising from the excess Fe content. Though the coercivity increased with subsequent heat treatments, the values are much smaller than expected and this can be attributed to the presence of second phase (Fe-oxide).

To know the distribution of Fe in the lattice and to identify the different phases present in the samples Mössbauer spectra was recorded. Fig. 4 shows the Mössbauer spectra of a) as synthesized and b) 600 °C heat-treated FePt NPs. Mössbauer spectrum of as synthesized sample was fitted with two distinct sub-spectra. One of the sub-spectra comprises of a sextet with hyperfine splitting (H_{hf}) value of 299 kOe which in turn indicates that FePt is present in the from an fcc structure [21]. The other sub-spectra are a doublet which can be attributed to a super-paramagnetic FePt phase.

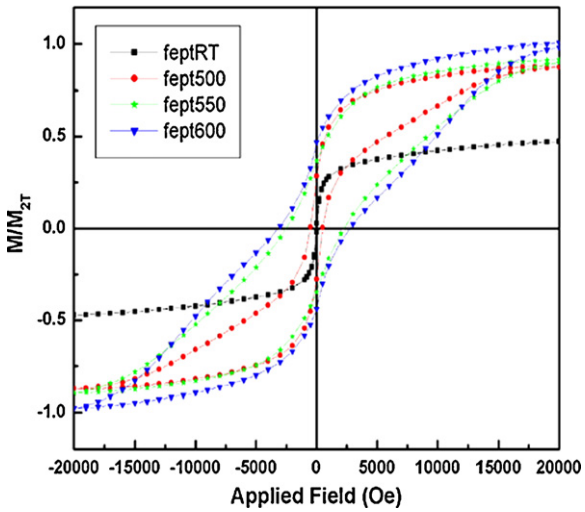

Fig. 3. *M–H* curves of FePt nanoparticles recorded at room temperature.

Table 1 shows the corresponding intensities along with their hyperfine splitting values of as-prepared and 600 °C heat-treated FePt NPs calculated from Mössbauer spectra. From Table 1 it can be observed that in case of as-prepared FePt NPs 70% of the particles exist in a super-paramagnetic state whereas only 30% exist in ferromagnetic disordered fcc form. This explains the narrow and sharp ferromagnetic like hysteresis loop observed while carrying out VSM. Fig. 4b consists of three different well resolved sub-spectra with one sextet and two doublets. The major phase being a sextet with a relative intensity of 57% and H_{hf} value of 285 kOe indicating that majority of the particles exists in the form of an ordered $L1_0$ structure. The doublet with second highest intensity of 23% shows that some of the NPs still exist in the super-paramagnetic phase and that the ordering is incomplete, which is concomitant with the XRD data. The third sub-spectra are a doublet which can be attributed to the presence of Fe in the oxidized form. Gener-

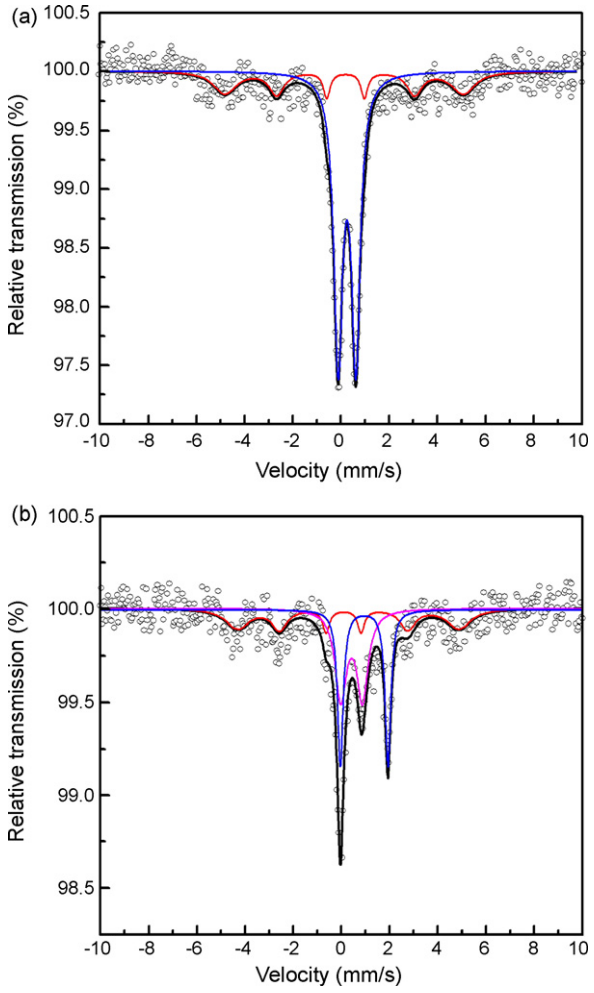

Fig. 4. Mössbauer spectra of (a) as synthesized and (b) 600 °C heat-treated FePt nanoparticles.

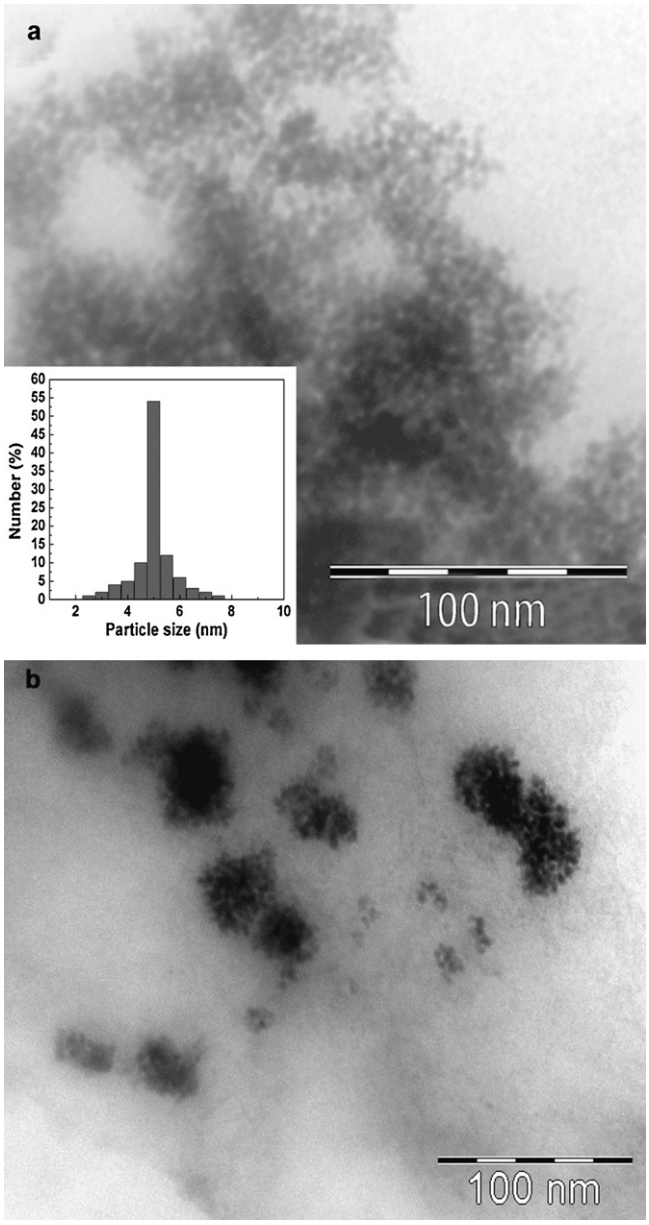

Fig. 5. TEM micrographs of (a) as-prepared FePt nanoparticles, inset its particle size distribution and (b) FePt nanoparticles heat treated at 600 °C.

ally two well resolved spectra appear for Fe_3O_4 but in this case as there are more than one oxide forms present in the sample an average doublet spectrum were obtained. The intensity of Fe-oxide state being 20% explains the phenomenon of multiphase hysteresis loops as well as the reduced coercivity values. One interesting fact could be observed from the above spectra is that in the as synthesized FePt NPs separate Fe-oxide state does not exist and it only appears on heat treatment, this indicates that on initial formation of NPs the excess iron is in the form of Fe^0, though subsequently it converts into an oxide form it still exists in an amorphous, superparamagnetic state. The same is also observed from XRD where initially only the disordered fcc structure is observed whereas the oxide peaks appear with subsequent heat treatments.

Fig. 5 shows the TEM micrographs of (a) as-prepared FePt NPs, inset its particle size distribution and (b) FePt NPs heat treated at 600 °C. From Fig. 5a it could be observed that nearly spherical and well dispersed FePt NPs have been obtained from the above method. The average particle size of as-prepared powders is 5 nm with a good particle size distribution as evidenced from the particle size distribution shown in the inset. Fig. 5b shows clusters of nanoparticles and this could be attributed to the fact that the FePt NPs are agglomerating during the process of heat treatment. This indicates that the Fe-oxide formed from excess Fe content could not efficiently control the agglomeration.

4. Conclusions

The above mentioned process produces Fe-rich FePt NPs with an average size of 5 nm having a narrow size distribution. Though a considerable coercivity of 3.2 kOe can be obtained with decreased Pt content, the excess Fe could not prevent coalescence during heat treatment instead lead to multiphase magnetic loops. The excess iron on synthesis is in the form of Fe^0 but picks up oxygen during the process of handling and heat treatment to convert into Fe_3O_4 and other oxide forms of iron. It is also observed that heat treatment at 600 °C for 1 h is not sufficient for complete conversion of FePt NPs to an ordered fct phase and therefore either the heat treatment time is to be prolonged or heat treated at elevated temperature. Further optimization process is in progress and will be reported subsequently.

Acknowledgements

This work was supported financially by the Defence Research and Development Organization (DRDO), Ministry of Defence, Government of India. We extend our thanks to the Director, DMRL, Hyderabad, for his keen interest in this work and for permission to publish these results. The authors are thankful to Dr. V. Chandrasekharan (AMG, DMRL, Hyderabad) for his interest and support while carrying out this work.

References

[1] Q.A. Pankhurst, J. Connolloy, S.K. Jones, J. Doboson, J. Phys. D: Appl. Phys. 36 (2003) R167–R181.
[2] H. Gu, P.-L. Ho, K.W.T. Tsang, L. Wang, B. Xu, J. Am. Chem. Soc. 125 (2003) 15702–15703.
[3] G. Viau, F. Fievet-Vincent, F. Fieĭvet, P. Toneguzzo, F. Ravel, O. Acher, J. Appl. Phys. 81 (1997) 2749–2754.
[4] Ph. Toneguzzo, G. Viau, O. Acher, F. Fievet-Vincent, F. Fievet, Adv. Mater. 10 (1998) 1032–1035.
[5] Y.H. Huang, H. Okumura, G.C. Hadjipanayis, D. Weller, J. Appl. Phys. 91 (2002) 6869–6871.
[6] P. Gibot, E. Tronc, C. Chaneac, J.P. Jolivet, D. Fiorani, A.M. Testa, J. Magn. Magn. Mater. 290–291 (2005) 555–558.
[7] S. Sun, C.B. Murray, D. Weller, L. Folks, A. Moser, Science 287 (2000) 1989–1992.
[8] T. Iwaki, Y. Kakihara, T. Toda, M. Abdullah, K. Okuyam, J. Appl. Phys. 94 (2003) 6807–6811.
[9] T.S. Vedantam, J.P. Liu, H. Zeng, S. Sun, J. Appl. Phys. 93 (2003) 7184–7186.
[10] M. Chen, T. Pica, Y.-B. Jiang, P. Li, K. Yano, J.P. Liu, A.K. Datye, H. Fan, J. Am. Chem. Soc. 129 (2007) 6348–6349.
[11] K.E. Elkins, T.S. Vedantam, J.P. Liu, H. Zeng, S. Sun, Y. Ding, Z.L. Wang, Nano Lett. 3 (2003) 1647–1649.
[12] Y.Z. Fu, X.D. Xiang, J. Dispers. Sci. Technol. 29 (2008) 861–865.
[13] H.L. Nguyen, L.E.M. Howard, G.W. Stinton, S.R. Giblin, B.K. Tanner, I. Terry, A.K. Hughes, I.M. Ross, A. Serres, J.S.O. Evans, Chem. Mater. 18 (2006) 6414–6424.
[14] S.S. Kang, D.E. Nickles, J.W. Harrell, J. Appl. Phys. 93 (2003) 7178–7180.
[15] K. Elkins, D. Li, N. Poudyal, V. Nandwana, Z. Jin, K. Chen, J.P. Liu, J. Phys. D: Appl. Phys. 38 (2005) 2306–2309.
[16] S. Saita, S. Maenosono, J. Phys. Condens. Matter 16 (2004) 6385–6394.
[17] J. Kim, C. Rong, Y. Lee, J.P. Liu, S. Sun, Chem. Mater. 20 (2008) 7242–7245.
[18] S. Kang, G.X. Miao, S. Shi, Z. Jia, D.E. Nikles, J.W. Harrell, J. Am. Chem. Soc. 128 (2006) 1042–1043.
[19] C. Liu, X. Wu, T. Klemmer, N. Shukla, D. Weller, A.G. Roy, M. Tanase, D. Laughlin, Chem. Mater. 17 (2005) 620–625.
[20] T.J. Klemmer, N. Shukla, C. Liu, X.W. Wu, E.B. Svedberg, O. Mryasov, R.W. Chantrell, D. Weller, M. Tanase, D.E. Laughlin, Appl. Phys. Lett. 81 (2002) 2220–2222.
[21] H.L. Wang, Y. Huang, Y. Zhang, G.C. Hadijipanayis, D. Weller, A. Simopoulos, J. Magn. Magn. Mater. 310 (2007) 22–27.